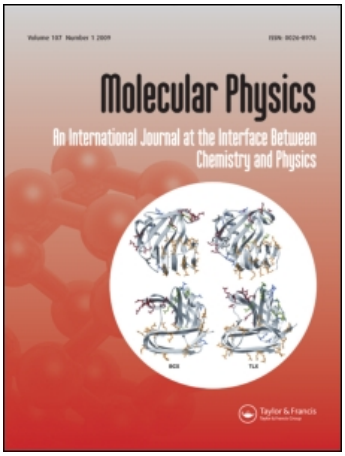

Molecular Physics
Publication details, including instructions for authors and subscription information:
http://www.informaworld.com/smpp/title~content=t713395160

Investigation of size effects on the physical properties of one-dimensional Ising models in nanosystems

Farid Taherkhani[ab]; Ebrahim Daryaei[c]; Gholamabbas Parsafar[a]; Alessandro Fortunelli[b]
[a] Department of Chemistry and Nanotechnology Center, Sharif University of Technology, Tehran, Iran [b] Istituto per i Processi Chimico-Fisici (IPCF) del CNR, Pisa, Italy [c] Department of Physics, Sharif University of Technology, Tehran, Iran

Online publication date: 13 February 2011

To cite this Article Taherkhani, Farid , Daryaei, Ebrahim , Parsafar, Gholamabbas and Fortunelli, Alessandro(2011) 'Investigation of size effects on the physical properties of one-dimensional Ising models in nanosystems', Molecular Physics, 109: 3, 385 — 395
To link to this Article: DOI: 10.1080/00268976.2010.524172
URL: http://dx.doi.org/10.1080/00268976.2010.524172

Molecular Physics
Vol. 109, No. 3, 10 February 2011, 385–395

Taylor & Francis
Taylor & Francis Group

RESEARCH ARTICLE

Investigation of size effects on the physical properties of one-dimensional Ising models in nanosystems

Farid Taherkhani[ac], Ebrahim Daryaei[b], Gholamabbas Parsafar[a]* and Alessandro Fortunelli[c]

[a]*Department of Chemistry and Nanotechnology Center, Sharif University of Technology, Tehran, Iran;* [b]*Department of Physics, Sharif University of Technology, Tehran, Iran;* [c]*Istituto per i Processi Chimico-Fisici (IPCF) del CNR, Via Giuseppe Moruzzi 1, I-56124, Pisa, Italy*

(*Received 18 July 2010; final version received 8 September 2010*)

Ising models in nanosystems are studied in the presence of a magnetic field. For a one-dimensional (1-D) array of spins interacting via nearest-neighbour and next-nearest-neighbour interactions we calculate the heat capacity, the surface energy, the finite-size free energy and the bulk free energy per site. The heat capacity versus temperature exhibits a common wide peak for systems of any size. A small peak also appears at lower temperatures for small arrays when the ratio of magnetic field spin interaction energy over the nearest-neighbour spin–spin interaction energy, f, is within $0 < f \leq 0.10$. The peak becomes smaller for longer array and eventually vanishes for long arrays, disappearing when the number of spins, N, is greater than 25 when only nearest-neighbour interactions are taken into account, and more than 14 when next-nearest-neighbour interactions are included as well. Ising models in which the nearest-neighbour interactions are ferromagnetic, while the next-nearest-neighbour interactions are either ferromagnetic or antiferromagnetic, are compared, and it is found that the reduced free energy in the former case exhibits a larger deviation from the bulk value.

Keywords: Ising model; nanosystem; surface energy; heat capacity; size effect

1. Introduction

Since the discovery of single-molecule magnets in 1993 [1,2], the synthesis and physical characterization of molecular nanomagnets have been one of the most active fields in molecular magnetism. Several reasons justify their importance: coexistence of classical properties attributed to bulk magnetic materials and quantum effects such as quantum tunneling of the magnetization [3,4] and phase interference [5], extremely long relaxation time of their magnetic moment, and potential use in molecular spintronics [6] and quantum computing [7]. Single chain magnets (SCMs) are an interesting class of molecular polymeric materials displaying slow relaxation of the magnetization. They provide, at low temperatures, a magnetic hysteretic behaviour for a single polymeric chain [8]. In 2001 Caneschi *et al*. observed a slow relaxation of the magnetization in a magnetically isolated cobalt (II) nitronyl nitroxide chain [9] and described the main experimental requirements to be fulfilled in the design of such one-dimensional (1-D) nanomagnets. 1-D magnetic models have attracted much interest in recent years, both because they are much easier to be treated theoretically than 2-D and 3-D models, and because of the discovery of several quasi 1-D magnetic materials. Most of these can be interpreted in terms of Ising models including a nearest-neighbour exchange interaction, whose sign determines the type of short range order: e.g. ferromagnetic in $CsNiF_3$ and antiferromagnetic in $(CH3)_4NMnCl_3$ [9]. As a matter of fact one finds a strong uniaxial Ising-type anisotropy and significant difference between intra-(J) and inter-chain (J') magnetic interactions in some materials. These magnetic nanowires are called single chain magnets [10,11]. The dark-brown crystals obtained by assembling of $[Mn(5\text{-}MeOsalen)(H_2O)]^+$ and$[(Tp)Fe(CN)_3]^-$ affords the 1-D zigzag chain $[(Tp)Fe(CN)_3Mn(5\text{-}MeOsalen).2CH_3OH]_n$ [$Tp^- =$ hydrotris (pyrazolyl) borate, 5-MeOsalen^{2-} = N, N' ethylenebis (5-methoxyysalicylideneiminate)]. An alternating topology was presented with J_a and J_b Mn-(III)–Fe(III) coupling parameters [12]. The anhydrous version of K-titanium alum, on the other hand, consists of layers of Ti^{3+} ions coordinated and interlinked to SO_4^{2-} anions, and provides a good realization of an $s = 1/2$ Ising model on the triangular lattice [13]. $KTi(SO_4)_2.H_2O$ is a

*Corresponding author. Email: parsafar@sharif.edu

ISSN 0026–8976 print/ISSN 1362–3028 online

DOI: 10.1080/00268976.2010.524172
http://www.informaworld.com

frustrated chain with $s=1/2$ with nearest-neighbour interaction ($J=9.462\,\mathrm{cm}^{-1}$) and a next-nearest-neighbour interaction J_1 with $\frac{J_1}{J}=0.291$ [14]. Other real systems that map onto this model include Cu [2-(2-aminomethyl)] Br_2 ($J_1/J=0.2$), [15] $(N_2H_5)CuCl_3$ ($J_1/J=4$), [16–17] $SrCuO_2$ ($J_1/J<-10$), [18–19] $LiCu_2O_2$ ($J_1/J=-1$), [20,21] $LiCuVO_4$ ($J_1/J=-0.78$), [22], and Li_2CuZrO_4 ($J_1/J=-0.3$) [23].

Many methods, such as renormalization group, finite-size scaling, cluster variational calculation [24], Monte Carlo method [25] and transfer matrix, have been used to investigate Ising models. In a previous study [26], a 2-D Ising model with a finite number of rows, n, and with the coordination number 4 for each site was investigated via transfer matrix techniques, and the exact thermodynamic properties were obtained. In this work the transfer matrix was solved for $n \leq 7$ in the presence of a magnetic field, for $n \leq 10$ in the absence of a magnetic field, and an analytical expression was obtained for the partition function [26]. The critical temperature of 2-D and 3-D Ising models as well as a 2-D Potts model was calculated by Ghaemi *et al*. [27]. The critical temperature for a 2-D Ising model was obtained for different types of lattice such as square, triangular and honeycomb lattices. [27]. The finite-size scaling approach based on the transfer matrix method was applied to calculate the critical temperature of an anisotropic two-layer Ising ferromagnetic on strips of r-wide site of square lattice [28]. The reduced internal energy per site was accurately calculated for the ferromagnetic case with nearest-neighbour couplings k_x, k_y in the $x-y$ plane and with an interlayer coupling k_z. The calculated configurational energies for different lattice sizes intersect at various points. The intersection point can be fitted to a power series in terms of the lattice size. The power series was used to obtain the critical temperature of the infinite two-layer lattice [28].

Surface and size effects are important in nanosystems and have a significant influence on the energy, which may not be extensive [29]. Exact solution for the thermodynamic functions of the randomly dilute $s=1/2$ nearest-neighbour Ising chain in a magnetic field was examined by Wortis [30], in which both site and bond impurities were treated. The system behaves non-analytically at $T=h=0$. The divergence of the pure-chain thermodynamics was replaced at non-zero dilution by essential singularities of the Griffiths type at which all functions are finite and infinitely differentiable [30].

The 1-D random Ising system of higher spin s has been considered in terms of power series of concentration of magnetic atoms, ρ. The specific heat and the zero-field susceptibility for $s=1$ and 3/2 and for arbitrary ρ were obtained. The specific heat of the random ternary system composed of two kinds of magnetic atoms and non-magnetic atoms was also obtained by Matsubara *et al*. [31]. Also the specific heat and the susceptibilities of the 1-D binary mixture and the binary Bethe lattice were given by Katsura and Matsubara [32]. One-dimensional dilute systems with nearest-neighbour interactions were studied in terms of power series of the concentration of magnetic atoms by Yoshimura and *et al*. [33] in which the recurrence relations among coefficients of the power series of the Ising systems were obtained. They studied systems with $s=1/2$, for which the specific heat, the susceptibility, and the magnetization of the ferromagnets and antiferromagnets were obtained. At low temperatures, three steps in the magnetization of antiferromagnetic systems were found. An Ising system of $s=1/2$ with nearest-neighbour (NN) and next-nearest neighbour (NNN) interactions was also studied by an extension of the method, and the specific heat was obtained at the zero magnetic field [33].

The problem of finite-size effects in $s=1/2$ Ising systems showing slow dynamics of the magnetization was investigated in presence of the diamagnetic impurities in a Co^{2+} radical chain by Bogani *et al*.[34]. The static magnetic properties have been measured and analyzed considering the peculiarities induced by the ferromagnetic character of the compound. The dynamic susceptibility shows that an Arrhenius law is observed with the same energy barrier for the pure and the doped compounds while the prefactor decreases, as theoretically predicted [34].

A study of finite-size effects on the static properties of a single-chain magnet was made by Bogani *et al*. [35]. The role of defects in the single-chain magnet CoPhOMe by inserting a controlled number of diamagnetic impurities was investigated by Pini *et al*. [35]. In an external applied field the system shows an unexpected behaviour, giving rise to a double peak in the susceptibility. The static thermodynamics properties of the randomly diluted Ising chain with alternating g-values were then obtained exactly via the transfer matrix approach. These results were compared to the experimental data of CoPhOMe, showing a qualitative agreement [35].

Also the Glauber dynamics was studied for 1-D system of [Mn2(saltmen)2Ni(pao)2(py)2](ClO4)2, (saltmen^{2-} *N,N*$^{-}$ –(1,1,2,2-tetramethylethylene) bis (salicylideneiminate); pao^{-} = pyridine-2-aldoximate; py = △pyridine) by Coulon *et al*. [36]. Above 2.7 K, the thermally activated relaxation time is mainly governed by the effect of magnetic correlations and the energy barrier experienced by each magnetic unit. Below 2.7 K, a crossover towards a relaxation regime is

observed that is interpreted as the manifestation of finite-size effects [36].

Multiplicity distributions, $P(n)$, for the 1-D Ising model with NN interactions have been shown to provide a successful and simple description of high-energy multiparticle productions. Huang extended the work to NNN interactions, and calculated the detailed shape of $P(n)$. He presented the numerical results for a finite lattice [37].

The magnetic structure of the edge-sharing cuprate compound Li2CuO2 was investigated with highly correlated *ab initio* electronic structure calculations. The NN- and NNN in chain magnetic interactions were calculated to be 142 and 222 K, respectively [38].

Measurement of the magnetic heat capacity, susceptibility and magnetization for $(CH_3)_4NCo(NO_2)_3$ (TMCON) which is an iso-structural compound with the Haldane compound $(CH_3)_4NNi(NO_2)_3$ (TMNIN) was done by Mito *et al.* [39]. From the analysis of these thermodynamic properties, they found that TMCON is a one-dimensional $s=1/2$ Ising system where the ferromagnetic NN interaction J_1 and the antiferromagnetic NNN interaction J_2 are competing. The value of J_1 is estimated to be $J_1/k_B = 28.0 \pm 4.0$ K (where k_B is the Bolzmann factor). It is confirmed that the results can be comprehensively explained only when we take $J_2 < 0$, although $J_2 = -0.22\ J_1$ estimated from the thermal analysis differs from $J_2 = -0.46\ J_1$ estimated from the magnetic susceptibility for the powdered sample [39].

Despite the previous work mentioned, the investigation of finite size effects in the case in which both NN and NNN interactions are simultaneously present has been rarely considered in the literature. On the contrary, information on thermodynamic quantities such as the heat capacity and the free energy would be valuable in connection with frustration effects in nano magnetic materials. Finite-size effects on the dynamics of the magnetization and the static magnetic properties of $s=1/2$ Ising systems were investigated for diamagnetic impurities in a Co^{2+} radical chain with NN interactions by Bogani *et al.* [34]. The single-chain magnet CoPhOMe, containing defects obtained by insertion of a controlled number of magnetic impurities, shows an unexpected behaviour in the presence of a magnetic field, giving rise to a double peak in the susceptibility [35]. As a matter of fact an impurity in a single chain magnet behaves as a perturbation. It seems interesting to investigate frustration effects in these systems and their connection with the unexpected behaviour of finite-size systems with NN and NNN interactions in small magnetic field (as a perturbation).

In the present work, we thus explore how the physics of 1-D Ising models is affected by the finite size of the system. In detail, we investigate the dependence of the heat capacity versus temperature as a function of the size of the system. Both NN and NNN interactions are included, and the effect of boundary conditions on the thermodynamic limit of 1-D Ising models is also investigated. For the case with only NN interactions, we use the transfer matrix technique to obtain an analytical solution for an array of any size. For an array with both NN and NNN interactions we derive analytical expressions for the partition function when the number of sites, N, is within$3 \le N \le 14$, both in the presence and in the absence of a magnetic field. If N is even and larger than 14, we derive an analytical expression for the partition function in the absence of a magnetic field, including both NN and NNN coupling interactions. However, in the presence of a magnetic field we could not find an analytical expression for the eigenvalues of the transfer matrix neither for a finite-size system nor for an infinite array. Therefore, a numerical solution is only reported for the infinite array at zero magnetic fields [40].

2. Calculation of surface energy and finite-size free energy

2.1. *Nearest-neighbour interactions in the presence of a magnetic field*

We start with the calculation of the partition function, Z, for the 1-D Ising model with NN interactions in the presence of a magnetic field:

$$Z = \sum_{\{s_1,s_2,s_3\ldots,s_N\}} \exp\{K(s_1s_2 + s_2s_3 + \ldots + s_{N-1}s_N + s_Ns_1) + h(s_1 + s_2 + \ldots s_N)\} \quad (1)$$

where $K = J/kT$, $s,h = H/kT$ are the reduced spin-spin nearest neighbour coupling energy, the spin of a site, and the reduced magnetic field, respectively. Equation (1) may be written as:

$$Z = \sum_{\{s_i\}} \exp\{Ks_1s_2 + h(s_1 + s_2)/2 + \ldots + Ks_Ns_1 + h(s_1 + s_N)/2 + Ks_Ns_1(1-1)\} \quad (2)$$

The partition function for this model can be computed via the transfer matrix method. The matrix element $T_{s_i,\,s_j}$ of the transfer matrix may be written as:

$$T_{si,\,sj} = \exp\left[K(s_is_j) + h(s_i + s_j)/2\right] \quad (3)$$

For free boundary conditions, the partition function in Equation (2) can be written as

$$Z = \sum_{\{s_i\}} \langle s_1 \left| T^{N-1} A T \right| s_1 \rangle \tag{4}$$

where,

$$A = \begin{pmatrix} e^{-Ks_1} & 0 \\ 0 & e^{Ks_1} \end{pmatrix} \tag{5}$$

By using the unitary matrix U, which diagonalizes T, the partition function can be written as

$$\begin{aligned} Z &= \sum_{\{s_i\}} \left\langle s_1 \left| T^{N-1} A T \right| s_1 \right\rangle \\ &= \sum_{\{s_i\}} \left\langle s_i \left| U U^{-1} T^{N-1} U U^{-1} A U U^{-1} T U U^{-1} \right| S_1 \right\rangle \end{aligned} \tag{6}$$

where U is

$$U = \begin{pmatrix} \cos\phi & \sin\phi \\ -\sin\phi & \cos\phi \end{pmatrix} \tag{7}$$

and φ is defined as,

$$\cot(2\phi) = e^{2K} \sinh(h) \tag{8}$$

The inverse matrix of U, U^{-1}, is

$$U^{-1} = \begin{pmatrix} \cos\phi & -\sin\phi \\ \sin\phi & \cos\phi \end{pmatrix} \tag{9}$$

The diagonalized matrix, T', is then given by

$$U^{-1} T^{N-1} U = (T')^{N-1} = \begin{pmatrix} \lambda_1^{N-1} & 0 \\ 0 & \lambda_2^{N-1} \end{pmatrix} \tag{10}$$

where

$$\lambda_1 = e^K \left(\cosh(h) + \sqrt{\sinh^2(h) + e^{-4K}} \right) \tag{11}$$

and

$$\lambda_2 = e^K \left(\cosh(h) - \sqrt{\sinh^2(h) + e^{-4K}} \right) \tag{12}$$

Operating the inverse of unitary matrix U^{-1} on spin up (+) gives,

$$U^{-1}|+\rangle = \begin{pmatrix} \cos & \phi \\ \sin & \phi \end{pmatrix} \tag{13}$$

Similar to Equation (13), operating the unitary matrix U^{-1} on spin (−) gives

$$U^{-1}|-\rangle = \begin{pmatrix} -\sin\phi \\ \cos\phi \end{pmatrix} \tag{14}$$

We thus obtain

$$U^{-1} A U = \begin{pmatrix} e^{-Ks_1}\cos^2\phi & e^{-Ks_1}\cos\phi\sin\phi \\ \quad + e^{Ks_1}\sin^2\phi & \quad - e^{Ks_1}\sin\phi\cos\phi \\ e^{-Ks_1}\cos\phi\sin\phi & e^{-Ks_1}\sin^2\phi \\ \quad - e^{Ks_1}\sin\phi\cos\phi & \quad + e^{Ks_1}\cos^2\phi \end{pmatrix} \tag{15}$$

We may define the matrix B as

$$B = U U^{-1} T^{N-1} U U^{-1} A U U^{-1} T U U^{-1} \tag{16}$$

The summation in Equation (6) on spin-up gives the following result

$$\begin{aligned} \langle +|B|+\rangle = {} & \lambda_1^N e^{-Ks_1}\cos^4\phi + (\sin^2\phi\cos^2\phi) e^{Ks_1} \\ & + \lambda_1\lambda_2^{N-1}\sin^2\phi\cos^2\phi e^{-Ks_1} \\ & - e^{Ks_1}\cos^2\phi\sin^2\phi + \lambda_1^{N-1}\lambda_2 e^{-Ks_1}\cos^2\phi\sin^2\phi \\ & - \lambda_1^{N-1}\lambda_2 e^{Ks_1}\sin\phi\cos^2\phi \\ & + \lambda_2^N e^{-Ks_1}\sin^3\phi + \lambda_2^N e^{Ks_1}\cos^2\phi\sin\phi \end{aligned} \tag{17}$$

and on spin-down gives

$$\begin{aligned} \langle -|B|-\rangle = {} & \lambda_1^N \left(e^{-Ks_1}\cos^2\phi\sin^2\phi + \sin^4\phi e^{Ks_1} \right) \\ & - \lambda_1^{N-1}\lambda_2 e^{-Ks_1}\sin^2\phi\cos^2\phi \\ & + \lambda_1^{N-1}\lambda_2 e^{Ks_1}\sin^2\phi\cos^2\phi \\ & - \lambda_1\lambda_2^{N-1}(\cos^2\phi\sin^2\phi e^{-Ks_1} \\ & + e^{Ks_1}\cos^2\phi\sin^2\phi) \\ & + \lambda_2^N \left(e^{-Ks_1}\sin^2\phi\cos^2\phi + e^{Ks_1}\cos^4\phi \right) \end{aligned} \tag{18}$$

Therefore, the sum of Equations (17) and (18) gives the partition function as

$$\begin{aligned} Z = \langle +|B|+\rangle + \langle -|B|- > \rangle = {} & e^{-K}\left(\lambda_1^N + \lambda_2^N\right) \\ & + \sin^2 2\phi \sinh(K)\left(\lambda_1^N + \lambda_2^N - \lambda_1\lambda_2^{N-1} + \lambda_1^{N-1}\lambda_2\right) \end{aligned} \tag{19}$$

By some rearrangement, Equation (19) can be written as

$$\begin{aligned} Z = {} & \lambda_1^N \left(\left(\sin^2 2\phi \sinh(K)\left(1 - \frac{\lambda_2}{\lambda_1}\right)\right) + e^{-K} \right) \\ & + \lambda_1^N \left(\sin^2 2\phi \sinh(K)\left(1 - \frac{\lambda_1}{\lambda_2}\right)\right) + e^{-K}\left(\frac{\lambda_2}{\lambda_1}\right)^N \end{aligned} \tag{20}$$

Therefore, the free energy, A, for the model in the presence of magnetic field reads as [30]

$$A=-Nk_BT\ln(\lambda_1)-k_BT\ln\left(\sin^2 2\phi\sinh(K)\left(1-\frac{\lambda_2}{\lambda_1}\right)+e^{-K}\right)-k_BT\ln\left(1+\frac{\sin^2 2\phi\sinh(K)\left(1-\frac{\lambda_1}{\lambda_2}\right)+e^{-K}}{\sin^2 2\phi\sinh(K)\left(1-\frac{\lambda_2}{\lambda_1}\right)+e^{-K}}\left(\frac{\lambda_2}{\lambda_1}\right)^N\right) \tag{21}$$

where k_B is the Boltzmann constant and T is absolute temperature.

From Equation (21), the Helmholtz free energy can be partitioned into three components: bulk, A_{bulk}, surface, A_{surface}, and finite-size, $A_{\text{finitessize}}$, which are given as

$$A_{\text{bulk}}=-Nk_BT\ln(\lambda_1) \tag{22}$$

$$A_{\text{surface}}=-k_BT\ln\left(\sin^2 2\phi\sinh(K)\left(1-\frac{\lambda_2}{\lambda_1}\right)+e^{-K}\right) \tag{23}$$

$$A_{\text{finitesize}}=-k_BT\ln\times\left(1+\frac{\sin^2 2\phi\sinh(K)\left(1-\frac{\lambda_1}{\lambda_2}\right)+e^{-K}}{\sin^2 2\phi\sinh(K)\left(1-\frac{\lambda_2}{\lambda_1}\right)+e^{-K}}\left(\frac{\lambda_2}{\lambda_1}\right)^N\right) \tag{24}$$

The first term is the bulk free energy which scales linearly with the size of system, the second term is the surface free energy which is independent of size, and the third term (the finite-size free energy) is contribution which depends on the size of the system. If $\lambda_2<\lambda_1$, then, defining the parameter a,

$$a=\frac{\sin^2 2\phi\sinh(K)\left(1-\frac{\lambda_1}{\lambda_2}\right)+e^{-K}}{\sin^2 2\phi\sinh(K)\left(1-\frac{\lambda_2}{\lambda_1}\right)+e^{-K}} \tag{25}$$

the third term on the right-hand-side of Equation (21) may be approximately written as

$$-k_BT\ln\left(1+\frac{\sin^2 2\phi\sinh(K)(1-\frac{\lambda_1}{\lambda_2})+e^{-K}}{\sin^2 2\phi\sinh(K)(1-\frac{\lambda_2}{\lambda_1})+e^{-K}}\left(\frac{\lambda_2}{\lambda_1}\right)^N\right)$$

$$\approx -k_BTa\left(\frac{\lambda_2}{\lambda_1}\right)^N$$

$$=-k_BTa\left(1-\frac{2\sqrt{\sin^2 h+e^{-4K}}}{\cosh(h)+\sqrt{\sinh^2(h)+e^{-4K}}}\right)^N$$

$$=-k_BTa\left(1-\frac{\frac{2}{\sin(2\phi)}}{e^{2K}\cosh(h)+\frac{1}{\sin(2\phi)}}\right)^N$$

$$=-k_BTa\left(1-\frac{2}{1+e^{2K}\cosh(h)\sin(2\phi)}\right)^N$$

If N is large and also $\frac{1}{1+e^{2K}\cosh(h)\sin(2\phi)}\to 0$, then

$$-k_BTa\left(1-\frac{2}{1+e^{2K}\cosh(h)\sin(2\phi)}\right)^N$$

$$\approx -k_BTa\exp\left(-\frac{2N}{1+e^{2K}\cosh(h)\sin(2\phi)}\right)$$

Therefore,

$$A_{\text{finitesize}}\approx -k_BTa\exp\left(-\frac{2N}{1+e^{2K}\cosh(h)\sin(2\phi)}\right) \tag{26}$$

We mention that Equations (21)–(24) were obtained by Wortis [30].

2.2. *Nearest-neighbour and next-nearest-neighbour interactions*

The Hamiltonian for the Ising model in the presence of a magnetic field is

$$H=\sum_i Js_is_{i+1}+\sum_i J_1s_is_{i+2}+h\sum_i s_i \tag{27}$$

where J and J_1 are the NN and NNN spin coupling interaction energies, respectively. The partition function can be calculated by using a computer program (Matlab software) for $N\le 14$. For instance, for $N=7$, the partition function is found to be

$$\begin{aligned}Z(7)=&\exp(7K+7K_1-7h)+7\exp(3K+3K_1-5h)\\&+7\exp(3K-K_1-3h)+7\exp(-\mathrm{K}+3\mathrm{K}_1-3h)\\&+7\exp(3\mathrm{K}-\mathrm{K}_1-h)+7\exp(-\mathrm{K}-\mathrm{K}_1-3h)\\&+14exp(-K-K_1-h)+7\exp(3K-K_1+h)\\&+7\exp(-K-5K_1-h)+7\exp(-5K+3K_1-h)\\&+14\exp(-K-K_1+h)+7\exp(-K-5K_1+h)\\&+7\exp(3K-K_1+3h)+7\exp(-5K+3K_1+h)\\&+7\exp(-K+3K_1+3h)+7\exp(-K-K_1+3h)\\&+7\exp(3K+3K_1+5h)+\exp(7K+7K_1+7h)\end{aligned}$$

For even values of N larger than 14, we may write the transfer matrix as (note that the transfer matrix is given in reference [40])

$$\begin{aligned}T(s_1^z,s_2^z,s_3^z,s_4^z)=&\exp\left[\frac{\beta J}{2}\left(s_1^zs_2^z+2s_2^zs_3^z+s_3^zs_4^z\right)\right]\\&\times\exp\left[\beta J_1\left(s_1^zs_3^z+s_2^zs_4^z\right)\right]\\&\times\exp\left[\frac{\beta H}{2}\left(s_1^z+s_3^z+s_2^z+s_4^z\right)\right]\end{aligned} \tag{28}$$

where $\beta=1/k_BT$.

Then, the transfer matrix in terms of $K=\frac{J}{k_BT}$ and $K_1=\frac{J_1}{k_BT}$ is

$$T_{s_1s_2,s_3s_4}=\begin{pmatrix} \exp(2K+2K_1+2h) & \exp(K+h) & \exp(-K+h) & \exp(-2K_1) \\ \exp(h-K) & \exp(-2K+2K_1) & \exp(-2K_1) & \exp(K-h) \\ \exp(K+h) & \exp(-2K_1) & \exp(-2K+2K_1) & \exp(-K-h) \\ \exp(-2K_1) & \exp(-K-h) & \exp(K-h) & \exp(2K+2K_1-2h) \end{pmatrix} \tag{29}$$

In the absence of a magnetic field, $h=0$, we can diagonalize the matrix to obtain its eigenvalues as follows:

$$\lambda_1 = 1/2\exp(-2K-4K_1)(\exp(6K_1)+2\exp(2K+2K_1) + \exp(4K+6K_1)+\exp(4K_1)(\exp(2K)+1) \times\sqrt{\left\{\begin{matrix}4\exp(2K)+\exp(4K_1)-2\exp(2K+4K_1)\\ +\exp(4K+4K_1)\end{matrix}\right\}} \tag{30-a}$$

$$\lambda_2 = 1/2\exp(-2K-4K_1)(\exp(6K_1)+2\exp(2K+2K_1) + \exp(4K+6K_1)-\exp(4K_1)(\exp(2K)+1) \times\sqrt{\left\{\begin{matrix}4\exp(2K)+\exp(4K_1)-2\exp(2K+4K_1)\\ +\exp(4K+4K_1)\end{matrix}\right\}} \tag{30-b}$$

$$\lambda_3 = 1/2\exp(-2K-4K_1)[\exp(6K_1)-2\exp(2K+2K_1) + \exp(4K+6K_1)-\exp(4K_1)(\exp(2K)-1) \times\sqrt{\left\{\begin{matrix}-4\exp(2K)+\exp(4K_1)-2\exp(2K+4K_1)\\ +\exp(4K+4K_1)\end{matrix}\right\}} \tag{30-c}$$

$$\lambda_4 = 1/2\exp(-2K-4K_1)[\exp(6K_1)-2\exp(2K+2K_1) + \exp(4K+6K_1)+\exp(4K_1)(\exp(2K)-1) \times\sqrt{\left\{\begin{matrix}-4\exp(2K)+\exp(4K_1)-2\exp(2K+4K_1)\\ +\exp(4K+4K_1)\end{matrix}\right\}} \tag{30-d}$$

Hence, the partition function is given as

$$Z=Tr[T]^{N/2}=\left(\lambda_1^{N/2}+\lambda_2^{N/2}+\lambda_3^{N/2}+\lambda_4^{N/2}\right) =\lambda_1^{N/2}\left(1+\frac{\lambda_2^{N/2}}{\lambda_1^{N/2}}+\frac{\lambda_3^{N/2}}{\lambda_1^{N/2}}+\frac{\lambda_4^{N/2}}{\lambda_1^{N/2}}\right) \tag{31}$$

where λ_1 is the largest eigenvalue of the matrix. In the thermodynamic limit $N\to\infty$, we have

$$Z=(\lambda_1)^{\frac{N}{2}} \tag{32}$$

Note that the diagonalization of the transfer matrix, given in Equation (29), is impossible in the general case. Therefore, we can only solve it numerically.

3. Results and discussion

3.1. *Systems with only nearest-neighbour interactions*

The exact reduced Helmholtz free energy of 1-D Ising model in the presence of a magnetic field, considering only NN interactions, can be obtained for any size in terms of the ratio of magnetic field-spin interaction energy to spin-spin coupling energy (f) Equation (21). The reduced surface free energy, $-A_{\text{surface}}/k_BT$, is given by Equation (23) for the model in the presence of a magnetic field, considering only the NN interactions, and is independent of N. The finite-size free energy, $A_{\text{finitsize}}$, is given in Equation (26). The heat capacity for this model is plotted in Figure 1 versus temperature for $N=3$, 5, 7, 9, 15, and 25 when $f=0.01$. In addition to a large peak, a small peak appears at low temperatures when $0<f\leq 0.1$ and $N\leq 25$, as shown for $f=0.01$ in Figure 1. In order to see the reason for appearance of the small peak, we have used the reduced Hamiltonian expression

$$H_{\text{reduce}}=\sum_i s_is_{i+1}+f\sum_i s_i \tag{33}$$

to calculate the energy levels of the model. They are compared in Figure 2(b) and (c) for two values of the parameter f, when $N=3$. As shown in this figure, when f is within 0 and 0.1 and N is not large ($N\leq 25$), the first exited state is very close to the ground state, a small amount of heat can be absorbed to transit the system between these two states. Such a transition gives rise to the small peak. Figure 2(c) clearly reveals the reason for the appearance of the small peaks in Figure 1(a) for small values of f ($N\leq 25$).

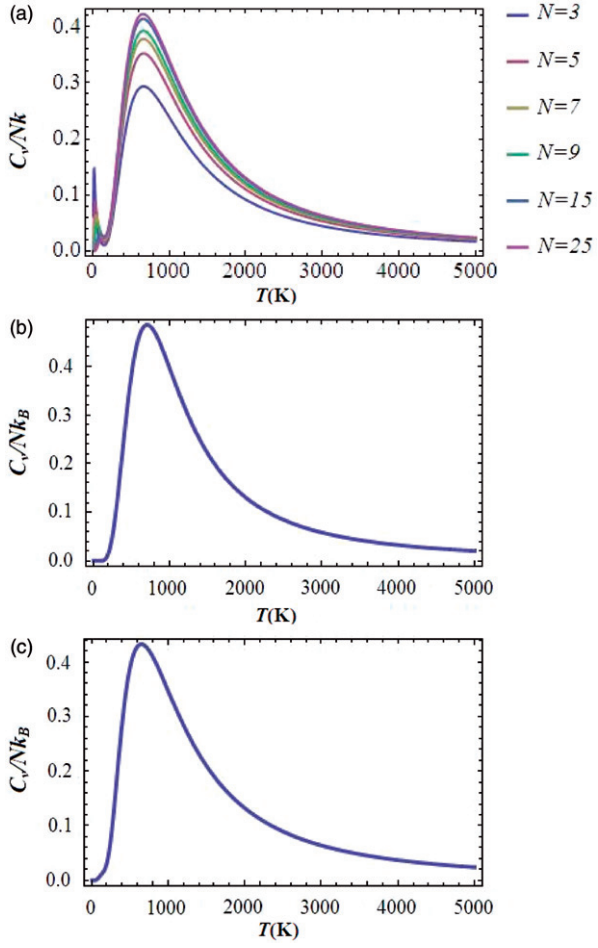

Figure 1. Reduced heat capacity versus temperature for the 1-D Ising model in the presence of a magnetic field, considering only nearest-neighbour interactions for (a) $N=3$, 5, 7, 9, 15, and 25 when $f=0.01$, (b) $N=3$ and $f=0.3$, and (c) $N=30$ and $f=0.01$.

3.2. *1-D Ising model in the presence of a magnetic field with nearest-neighbour and next-nearest-neighbour interactions*

3.2.1. *Thermodynamic limit including periodic boundary conditions*

If periodic boundary conditions (PBC) are applied, the finite-size free energy does not significantly depart from the bulk free energy even for small values of N, and rapidly approaches its bulk value. The calculated reduced free energy versus $K=\frac{J}{k_BT}$ for $N=3$, 4, and 5, competition parameter $J_1/J=0.2$ and $f=0.2$ is presented in Figure 3. Due to the fact that there is no analytical solution for the transfer matrix of the model in the presence of a magnetic field, to obtain the thermodynamic limit we have solved the transfer matrix given in Equation (28) numerically to find its maximum eigenvalue. The calculated partition function is used to calculate the free energy, which is shown in Figure 3.

3.2.2. *Heat capacity*

When applying PBC in the presence of both NN and NNN interactions, the analytical expression can be used to calculate the heat capacity for given values of $N\leq 14$, J_1/J, and f. The calculated results when $\frac{J_1}{J}=0.2$ and $\frac{h}{J}=f=0.01$ for the case of ferromagnetic interactions with both NN and NNN are plotted in Figure 4, for given values of N. According to Figure 4, in addition to a wide peak, again there is a small peak at low temperatures when $0<f\leq 0.1$ and $N\leq 14$. The small peak disappears for larger values of N. The reason for appearance of the small peak is exactly the same as that discussed in the case of NN interactions only (see Figure 1). The energy levels may be calculated from the reduced Hamiltonian expression:

$$H_{\text{reduce}}=\sum_i s_is_{i+1}+J_1/J\sum_i s_is_{i+2}+f\sum_i s_i \qquad (34)$$

The small peak disappears also in strong magnetic field and/or for large antiferromagnetic NNN interactions.

When $N=3$, $J=10$ and $f=0.01$, the heat capacity versus temperature for given values of J_1 (both positive and negative values) is presented in Figure. 5. As shown in this figure, the peak of heat capacity in the case of antiferromagnetic interactions appears at a lower temperature, compared to the case with ferromagnetic NNN interactions.

3.3. *Thermodynamic limit for free boundary condition with NN and NNN ferromagnetic interactions*

In the case of free boundary conditions, the effect of the finite size of the system may be quite significant, because both surface and finite-size components of the free energy are sizeable. The reduced Helmholtz free energy of 1-D Ising model in the presence of a magnetic field has been calculated for different sizes in terms of NN coupling energy (K), when $J_1/J=0.2=f$, Figure 6. This figure indicates that the reduced free energy increases with N, but its increase slows down for larger values of N. The free energy approaches the bulk value when N becomes large. In the thermodynamic limit, the reduced free energy is determined by the largest eigenvalue of the transfer matrix of Equation (29). The maximum eigenvalue is calculated numerically when $J_1/J=0.2=f$, and this result is used to calculate the

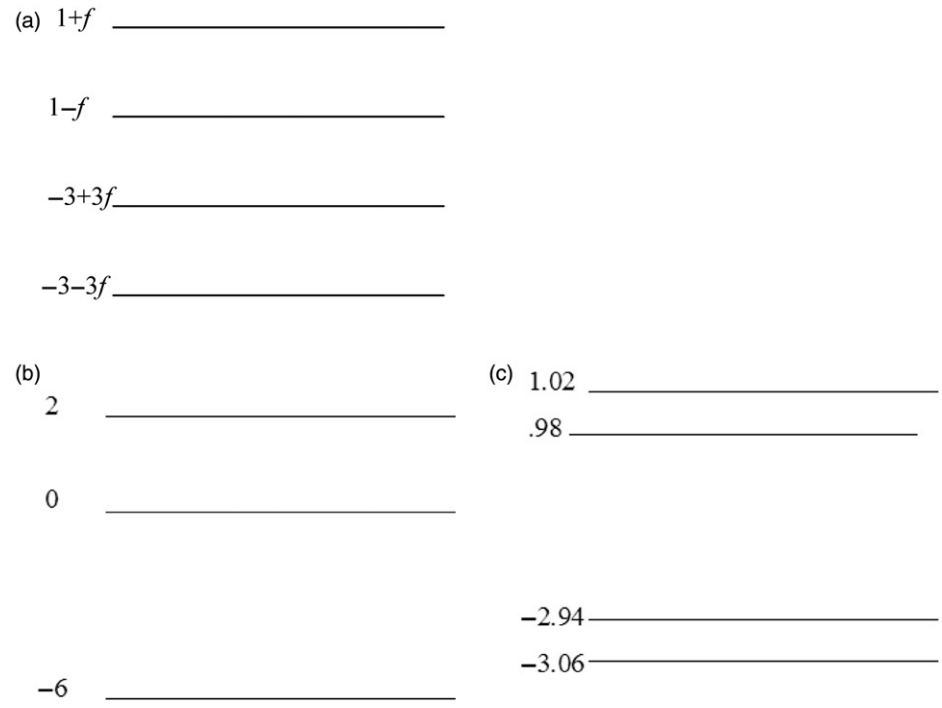

Figure 2. Energy levels for the 1-D Ising model with NN interactions and $N=3$ in the presence of a magnetic field: (a) as a function of f and for (b) $f=1$ and (c) $f=0.02$.

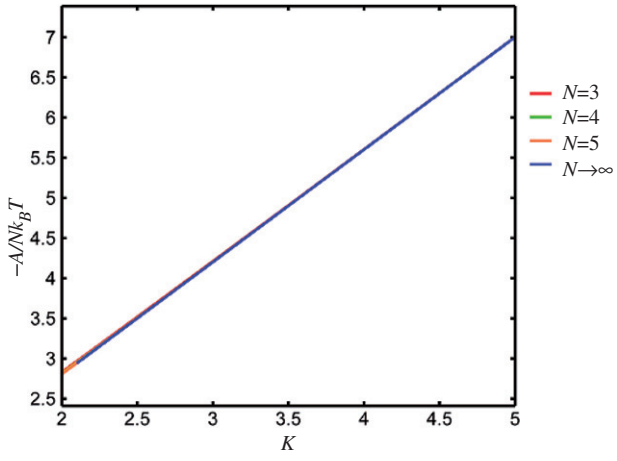

Figure 3. Reduced free energy versus $K=J/k_BT$ in the presence of NNN interactions, when $J_1/J=0.2$ and $f=0.2$, for $N=3$, 4, 5 and ∞. Periodic boundary conditions are applied.

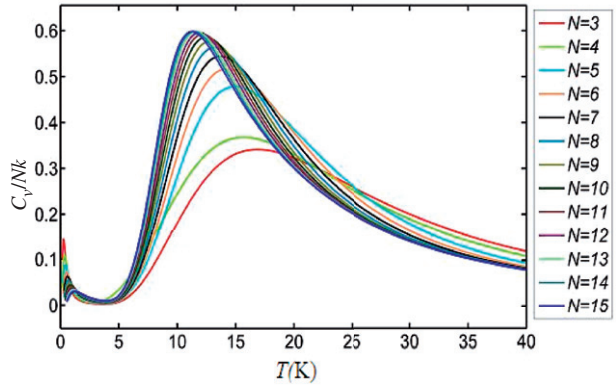

Figure 4. Reduced heat capacity versus temperature in the presence of NNN interactions, when PBC are applied, for $J_1/J=0.2$, $f=0.01$, and given values of N.

free energy in terms of K, as shown in Figure 6. For small values of K, we can easily calculate the relative difference in free energy for the finite model and the bulk, (ΔA), which is shown in Figure 7. The relative difference ΔA increases with K, but to a lesser extent for large values of N.

3.4. *Thermodynamic limit for NN ferromagnetic and NNN antiferromagnetic interactions*

Size effects on the free energy can be investigated when NN and NNN interactions are ferromagnetic and antiferromagnetic, respectively. In the thermodynamic limit, the reduced free energy is determined by the largest eigenvalue of the transfer matrix of Equation (29). The maximum eigenvalue was numerically calculated for

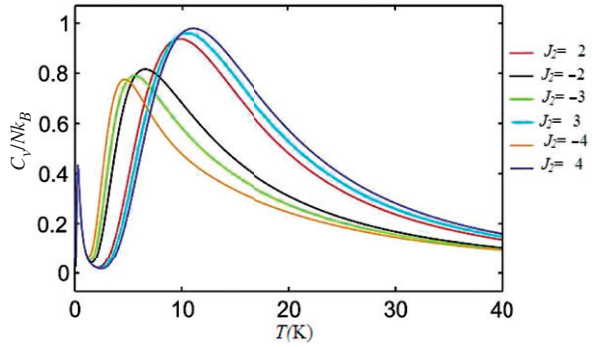

Figure 5. Reduced heat capacity versus temperature in the presence of NNN interactions when $J_1 = 10$, $J_2 = 2$, -2, 3, -3, 4, -4, $f = 0.01$, and $N = 3$.

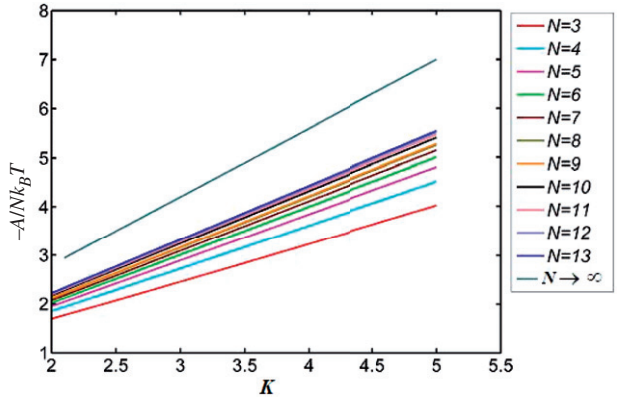

Figure 6. Reduced free energy in the presence of NNN interactions as a function of the reduced NN interaction energy (K) when $f = J_1/J = 0.2$ and for given values of N, in the case of free boundary conditions.

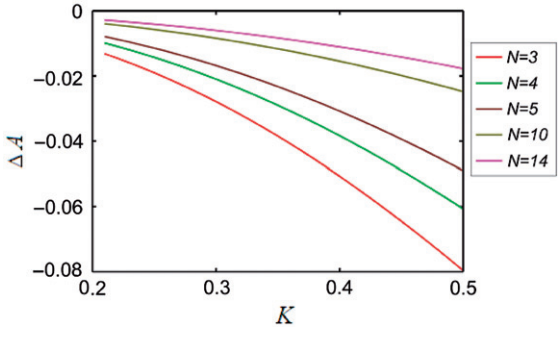

Figure 7. Relative difference in free energy of finite-size and bulk systems in the presence of NNN interactions in terms of the reduced NN interaction energy (K) for given values of N, when $f = J_1/J = 0.20$.

$f = 0.20$ and $J_1/J = -0.20$. The results are used to calculate the free energy in terms of K. By comparing Figuers 7 and 8, one can see that in the latter case the system approaches the thermodynamic limit for much

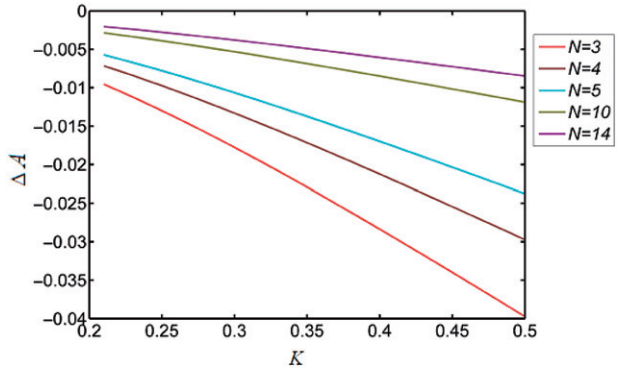

Figure 8. Relative difference in free energy of the finite-size and bulk systems in the presence of NNN interactions in terms of K, when $f = 0.20$ and $J_1/J = -0.20$ for given values of N.

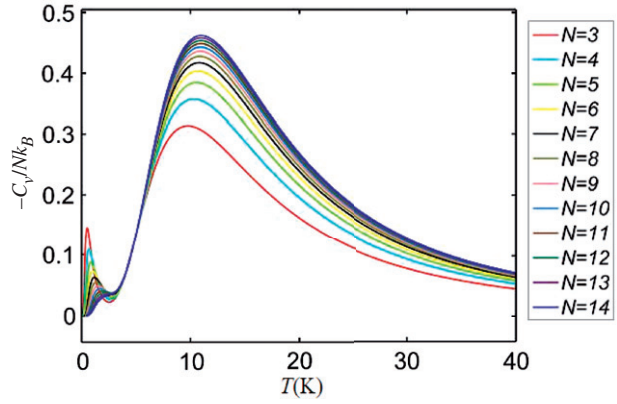

Figure 9. Reduced heat capacity versus temperature for the Ising model in the presence of NNN interactions, when free boundary conditions are applied, for $J_1/J = 0.2$, $f = 0.01$, and given values of N.

smaller values of N, compared to the case in which both interactions are ferromagnetic.

3.4.1. *Heat capacity*

Applying free boundary conditions in the presence of both NN and NNN interactions, an analytical expression is used to calculate the heat capacity for given values of $N \leq 14$, $J_1/J = 0.2$ and $f = 0.2$, and the results are shown in Figure 9. As can be seen from Figure 9, one finds again a small peak at low temperatures when $0 < f \leq 0.1$ and $N \leq 14$. However, for larger values of N, the small peak disappears, as well as for strong magnetic fields and for large antiferromagnetic NNN interactions.

4. Conclusions

A finite 1-D array of spins interacting via nearest-neighbour and next-nearest-neighbour interactions was considered in the present work. The heat capacity, the surface energy, the finite-size free energy and the bulk free energy per site have been calculated for this system, and analyzed as function of the size of the system, the relative strength of the applied magnetic field and the ratio of nearest-neighbour to next-nearest-neighbour interactions. The main conclusions that can be drawn from such an analysis are the following.

The heat capacity versus temperature exhibits a common wide peak for systems of any size, but an extra peak also appears for finite systems in the presence of not too strong magnetic fields. The appearance of this extra peak is due to the small energy separation between the ground and the first excited state, when the magnetic field and the size of system are both small (as schematically illustrated in Figure 2). The small peak arises because of the small quantity of energy (heat) needed to transit the system between the low-energy states. However, either for large values of N or in strong magnetic fields the small peak disappears (see Figure 1).

The use of PBC leads to a small size dependence of the free energy as compared to the case with free boundary conditions (compare Figures 3 and 6). It is worthwhile to note that Ogly [41] presented an analytical solution for the model in presence of a magnetic field, when the NN and NNN interactions are both taken into account. The accuracy of his analytical solution has been recently questioned [42].

Acknowledgements

Financial support from Sharif University of Technology and the SEPON project within the ERC Advanced Grants is gratefully acknowledged.

References

[1] R. Sessoli, D. Gatteschi, A. Caneschi and M.A. Novak, Nature **365**, 141 (1993).
[2] D. Gatteschi, R. Sessoli and J. Villain, *Molecular Nanomagnets* (Oxford University Press, Oxford, 2006).
[3] L. Thomas, F. Lionti, R. Ballou, D. Gatteschi, R. Sessoli and B. Barbara, Nature **383**, 145 (1996).
[4] J.R. Friedman, M.P. Sarachik, J. Tejada and R. Ziolo, Phys. Rev. Lett. **76**, 3830 (1996).
[5] W. Wernsdorfer and R. Sessoli, Science **284**, 133 (1999).
[6] L. Bogani and W. Wernsdorfer, Nat. Mater. **7**, 179 (2008).
[7] M.N. Leuenberger and D. Loss, Nature **410**, 789 (2001).
[8] L. Bogani, A. Vindigni, R. Sessoli and D. Gatteschi, J. Mater. Chem. **18**, 4750 (2008).
[9] A. Caneschi, D. Gatteschi, N. Lalioti, C. Sangregorio, R. Sessoli, G. Venturi, A. Vindigni, A. Rettori, A. Pini, M.G. Novak and M.A. Angew, Chem. Int. Ed. **40**, 1760 (2001).
[10] R. Clérac, H. Miyasaka, M. Yamashita and C. Coulon, J. Am. Chem. Soc. **124**, 12837 (2002).
[11] C. Coulon, H. Miyasaka and R. Clerac, Struct. Bonding (Berlin). **122**, 163 (2006).
[12] Shi. Wang, M. Ferbinteanu and M. Yamashita, Inorg. Chem. **46**, 610 (2007).
[13] S.T. Bramwell, S.G. Carling, C.J. Harding, K.D.M. Harris, B.M. Kariuki, L. Nixon and I.P. Parkin, J. Phys. Condens. Matter **8**, 123 (1996).
[14] G.J. Nilsen, H.M. Ronnow, A.M. Lauchli, F.P.A. Fabbiani, J. Sanchez-Benitez, K.V. Kamenev and A. Harrison, Chem. Mater. **20**, 8 (2008).
[15] H. Kikuchi, H. Nagasawa, Y. Ajiro, T. Asano and T. Goto, Physica B **284**, 1631 (2000).
[16] D.B. Brown, J.A. Donner, J.W Hall, S.R. Wilson, R.B. Wilson, D.J. Hodgson and W.E. Hatfield, Inorg. Chem. **18**, 2635 (1979).
[17] N. Maeshima, M. Hagiwara, Y. Narumi, K. Kindo, T.C. Kobayashi and K. Okunishi, J. Phys. Condens. Matter **15**, 3607 (2003).
[18] I.A. Zaliznyak, H. Woo, T.G Perring, C.L. Broholm, C.D. Frost and H. Takagi, Phys. Rev. Lett. **93**, 087202 (2004).
[19] M. Matsuda and K.J. Katsumata, Magn. Mater. **140**, 1671 (1995).
[20] S.L. Drechsler, N. Tristan, R. Klingeler, B. Büchner, J. Richter, J. Mlek, O. Volkova, A. Vasiliev, M. Schmitt, A. Ormeci, C. Loison, W. Schnelle and H. Rosner, J. Phys. Condens. Matter **19**, 145230 (2007).
[21] T. Masuda, A. Zheludev, A. Bush, M. Markina and A. Vasiliev, Phys. Rev. Lett. **92**, 177201 (2004).
[22] M. Enderle, C. Mukherjee, B. Fåk, R.K. Kremer, J.M. Broto, H. Rosner, S.L. Dreschler, J. Richter, J. Malek, A. Prokofiev, W. Assmus, S. Pujol, J.L. Ragazzoni, H. Rakoto, H. Rheinstädter and H.M. Rønnow, Europhys. Lett. **70**, 237 (2005).
[23] S.L. Drechsler, O. Volkova, A.N. Vasiliev, N. Tristan, J. Richter, M. Schmitt, H. Rosner, J. Mlek, R. Klingeler, A. Zvyagin and B. Büchner, Phys. Rev. Lett. **94**, 039705 (2004).
[24] R. van der Haegen and R. Luyckx, Mol. Phys. **49**, 849 (1983).
[25] J.R. Recht and A.Z. Panagiotopoulos, Mol. Phys. **80**, 843 (1993).
[26] Sh. Ranjbar and G.A. Parsafar, J. Phys. Chem. B **103**, 7514 (1999).
[27] M. Ghaemi, G.A. Parsafar and M. Ashrafizaadeh, J. Phys. Chem. B **105**, 10355 (2001).

[28] M. Ghaemi, M. Ghannadi and B. Mirza, J. Phys. Chem. B **107**, 10355 (2003).
[29] R. Salazar, A.R. Plastino and R. Toral, J. Europhys. B **17**, 679 (2000).
[30] M. Wortis, Phys. Rev. B **10**, 4665 (1974).
[31] F. Matsubara and K. Yoshimura, Progress of Theoretical Physics **50**, 1824 (1973).
[32] F. Matsubara and S. Katsura, Can. J. Phys. **52**, 120 (1974).
[33] F. Matsubara, S. Katsura and K. Yoshimura, Can. J. Phys. **51**, 1053 (1973).
[34] L. Bogani, A. Caneschi, M. Fedi, D. Gatteschi, M. Massi, M.A. Novak and M.G. Pini, Phys. Rev. Lett. **92**, 207204 (2004).
[35] L. Bogani, R. Sessoli, M.G. Pini, A. Rettori, M.A. Novak, P. Rosa, M. Massi, M.E. Fedi, L. Giuntini, A. Caneschi and D. Gatteschi, Phys. Rev. B **72**, 064406 (2005).
[36] C. Coulon, R. Clerac, L. Lecren, W. Wernsdorfer and H. Miyasaka, Phys. Rev. B **69**, 132408 (2004).
[37] D. Huang, Physica A **260**, 106 (1998).
[38] C. Graaf, P.R. Moreira, F. Illas, O. Iglesias and A. Labarta, Phys. Rev. B **66**, 014448 (2002).
[39] M. Mito, M. Ito, T. Kawae, M. Hitaka, H. Deguchi, S. Takagi and K. Takeda, J. Phys. Soc. Jpn **64**, 4402 (1995).
[40] M.G. Pini and A. Rettori, Phys. Rev. B **48**, 3240 (1993).
[41] K. Ogly, Phase Transition **74**, 353 (2001).
[42] F. Taherkhani, E. Daryaei, H. Abroshan, H. Akbarzadeh, G.A. Parsafar and A. Fortunelli, Phase Transition in press.